

We are IntechOpen, the world's leading publisher of Open Access books Built by scientists, for scientists

5,800

Open access books available

142,000

International authors and editors

180M

Downloads

Our authors are among the

154

Countries delivered to

TOP 1%

most cited scientists

12.2%

Contributors from top 500 universities



WEB OF SCIENCE™

Selection of our books indexed in the Book Citation Index
in Web of Science™ Core Collection (BKCI)

Interested in publishing with us?
Contact book.department@intechopen.com

Numbers displayed above are based on latest data collected.
For more information visit www.intechopen.com



Salp Swarm Optimization with Self-Adaptive Mechanism for Optimal Droop Control Design

*Mohamed A. Ebrahim, Reham M. Abdel Fattah,
Ebtisam M. Saied, Samir M. Abdel Maksoud
and Hisham El Khashab*

Abstract

The collaboration of the various distributed generation (DG) units is required to meet the increasing electricity demand. To run parallel-connected inverters for microgrid load sharing, several control strategies have been developed. Among these methods, the droop control method was widely accepted in the research community due to the lack of important communication links between parallel-connected inverters to control the DG units within a microgrid. To help to solve the power-sharing process, keep to frequency and voltage constrained limits in islanded mode microgrid system. The parameter values must therefore be chosen accurately by using the optimization technique. Optimization techniques are a hot topic of researchers; hence This paper discusses the microgrid droop controller during islanding using the salp swarm inspired algorithm (SSIA). To obtain a better fine microgrid output reaction during islanding, SSIA-based droop control is used to optimally determine the PI gain and the coefficients of the prolapse control. The results of the simulation show that the SSIA-based droop control can control the power quality of the microgrid by ensuring that the keep to frequency and voltage constrained limits and deviation and proper power-sharing occurs during the microgrid island mode during a load change.

Keywords: Droop control, microgrid, salp swarm inspired algorithm, distributed generation, power-sharing

1. Introduction

In the last decade, the electricity demand was increase and shortly, the electricity demand will be expected to rise significantly [1]. To meet this projected demand, there is a trend towards renewable energy sources to be used because they are environmentally sound and are considered economically better [1]. This transition in electricity generation from conventional to renewable energy sources (RES) [2]. This has culminated in the development of small-scale power generation systems named microgrids [2]. A microgrid that involves local loads and Distributed generation sources (DGs) [3]. DG systems are ideal for highly reliable electrical power

supply [3]. Various types of energy resources are currently available, such as wind turbines (WTs), photovoltaic systems (PVS), fuel cells (FC) [4]. It is difficult to connect these renewable resources directly to a utility grid [5]. To solve this problem, the microgrid is used to make the interface between the utility grid and distributed renewable resources [3]. Microgrids must be worked in the grid-connected mode as well as island mode contingency [3]. The power produced from most renewable resources is direct current (DC) but the utility grid is alternating current (AC). The inverter must be used to convert DC to AC. Therefore, an inverter is the main microgrid element [3]. In a microgrid, there are working Inverter parallel. The Inverters parallels are guaranteed to high reliability. Because if an inverter fails, the remaining modules can still supply the necessary power to the load [3]. The inverters control is intended to deliver the active and reactive energy while preserving the variability in frequency and voltage within the allowable limits [6]. To control inverters used the droop control technique. The droop control technique provides power-sharing, voltage and frequency constrained limits [7]. Such droop controllers are tuned with identical parameters in the d-axis and q-axis by trial and error method [8]. Nonetheless, in obtaining optimum parameters or even the right outcomes, this method has a major limitation.

Before human existence on this planet, nature used evolution to constantly solve challenging problems. The researchers inspired a solution based on nature to solve the difficult problems and challenges facing them. In 1977, Holland introduced a revolutionary idea in the field of optimization when evolutionary ideas in nature were modeled in computers to solve optimization problems [9]. The emergence of a new form of heuristic algorithm is Genetic Algorithms (GA), which is the most common and famous [10]. Opening the door for researchers to research and study to find new ways to solve the problems and challenges facing them in different fields.

Heuristic algorithms treat the problem as a black square with a combination of inputs and outputs. Their inputs are the problem variables and the outputs are the goals or objectives. A heuristic search begins with the formation of a collection of randomized inputs as the solution to the problem. The search is followed by analyzing each solution, monitoring objective values, and modifying /mixing/ developing output-based solutions. These steps will be repeated until solve the problem [9].

Researchers have a propensity to use optimization algorithms to overcome many engineering problems and challenges, but there is a question for researchers “Is there an only technique of optimization that can solve all problems? “. Lately, several types of algorithms have emerged such as Harris hawks optimization (HHO) [11], Salp Swarm Inspired Algorithm (SSIA) [12–14], grasshopper optimization algorithm (GOA) [1, 15], Sine Cosine Algorithm (SCA), Whale Optimization Algorithm (WOA) [16–18], Moth-Flame Optimization Techniques [19], Gray Wolf Algorithm (GWO) [20–22], Ant Lion Optimizer (ALO) [23], Moth-Flame Optimization algorithm (MFO) [24, 25], particle swarm optimization (PSO) [26, 27] and Dragonfly Algorithm (DA) [28] were the outcome of GA’s success. Any heuristic algorithm is flawed and the output is influenced by its limitations.

But there’s a fundamental question of “why do researchers keep discovering or developing new algorithms?”. There is a theory that explains the answer to this question, which is called the rule of no free lunch (NFL) [23]. Logically, this principle shows that no one can suggest an algorithm to solve all optimization issues. This does not mean that the effectiveness of a type of algorithm in solving a particular set of problems is that it can solve all the optimization problems. The NFL principle enables researchers to suggest new optimization algorithms or to enhance existing algorithms to solve problem subtypes in various fields [23].

The study proposes an SSIA-based controller to optimize the parameters of the PI controller and droop control coefficients under load change conditions to control the voltage, frequency and power-sharing of an islanded MG.

2. Salp swarm inspired algorithm (SSIA)

There are several swarm algorithms, many of them inspired by food search behavior, that have emerged so far. A new swarm intelligence technique known as SSIA inspired by the action of salp was proposed by Mirjalili et al. [29]. Salps are from the Salpidae family. Salp is described as a body shaped like a barrel with a transparent body. Salps are strongly jellyfish-like. The salp environment in which he lives is difficult to reach and also difficult to provide this environment in the laboratory, so it is difficult to preserve. Biological studies of salp are therefore in its early stages. The salp forms the salp chain, a swarm that lives in the deep ocean [30]. The chains of salp are made up of two groups: leaders and followers. The leader is at the front of the chain, but the follower is named the remainder of salp. In an n-dimensional search space where n is the number of variables of a given problem, the location of salps is. It can be observed from the nature of the salp's actions that the leader salp goes around the source of food and the followers follow the leader. The leader changes his position in every iteration and the followers adopt it when finding food. In **Figure 1** The form and nature of the salp swarm.

Figure 2 illustrates the leader and follower's movement around the food. In a two-dimensional matrix named x, the location of all salps is stored. It is also believed that in the search space there is a food source called F as the target of the swarm. To alter the location of the Leader, the following equation is proposed [29]:

$$x_j^1 = \begin{cases} F_j + c_1((ub_j - lb_j)c_2 + lb_j)c_3 \geq 0 \\ F_j - c_1((ub_j - lb_j)c_2 + lb_j)c_3 < 0 \end{cases} \quad (1)$$

where

x_j^1 : first Salp (leader) position in the jth dimension,

F_j : food source position of the jth dimension,

ub_j : upper bound of jth dimension,

lb_j : lower bound of jth dimension,

l : current iteration,

L : maximum number of iterations,

c_1 , c_2 , and c_3 : random numbers uniformly generated in the interval of [0,1].

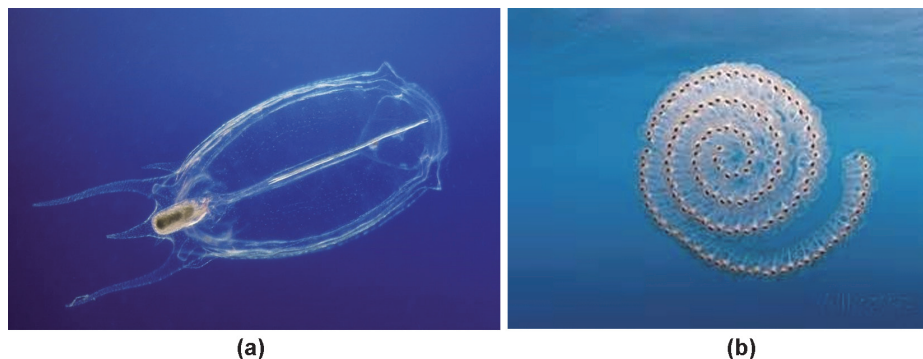


Figure 1. Shape and structure of salp swarm in the deep ocean. (a) Single salp, and (b) single salp chain.

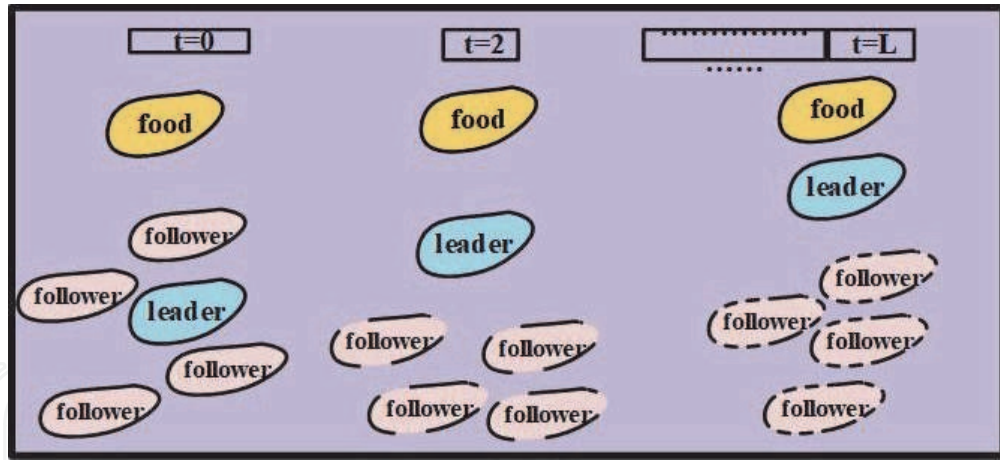


Figure 2.
The swarm of Salps (Salps chain) [31].

x_j^i : position of n^{th} follower salp in i^{th} dimension.

c_1 is a significant coefficient that balances exploration and exploitation. The following equation is used to estimate c_1 [12, 32]:

$$c_1 = 2e^{-\left(\frac{t}{L}\right)^2} \quad (2)$$

Newton's law of motion will be used to update the position of the followers as follows:

$$x_j^i = \frac{1}{2} ct^2 + \lambda_0 t \quad (3)$$

Where $I \geq 2$ and x_j^i shows the position of i^{th} follower salp in j^{th} dimension, t is time, λ_0 is the initial speed, and $c = \frac{\lambda_{\text{final}}}{\lambda_0}$ where $\lambda = \frac{x-x_0}{t}$.

For restructuring, in an optimization problem, it can be inferred that t is the iteration; this equation can be represented as follows:

$$x_j^i = \frac{1}{2} (x_j^i + x_j^{i-1}) \quad (4)$$

The advantages of SSIA:

1. A strong convergence acceleration.
2. Expedited method for providing excellent solutions.
3. Compatible with many types of optimization problems
4. A globally effective scheme to look for
5. Suitable for a broad search field.
6. In concept and implementation for related applications, SSA is simple.
7. A few parameters for tuning.

The SSIA pseudo-code algorithm is shown in **Figure 3**. **Figure 4** Performs flowchart for the SSIA.

```

Initialize the salp population  $x_i$  ( $i=1, 2, \dots, n$ ) considering  $ub$  and  $lb$ 
while (end condition is not satisfied)
    Calculate the fitness of each search agent (salp)
    F = the best search agent
    SSIA  $c_1$  calculated by Eq. (2)
    for each salp ( $x_i$ )
        if ( $i=1$ )
            SSIA the position of the leading salp calculation by Eq. (3)
        else
            Modify the position of the follower salp by Eq. (4)
        end
    end
    Amend the salps based on the upper and lower bounds of variables
end
return F
    
```

Figure 3.
 Pseudo code of the SSIA algorithm [12].

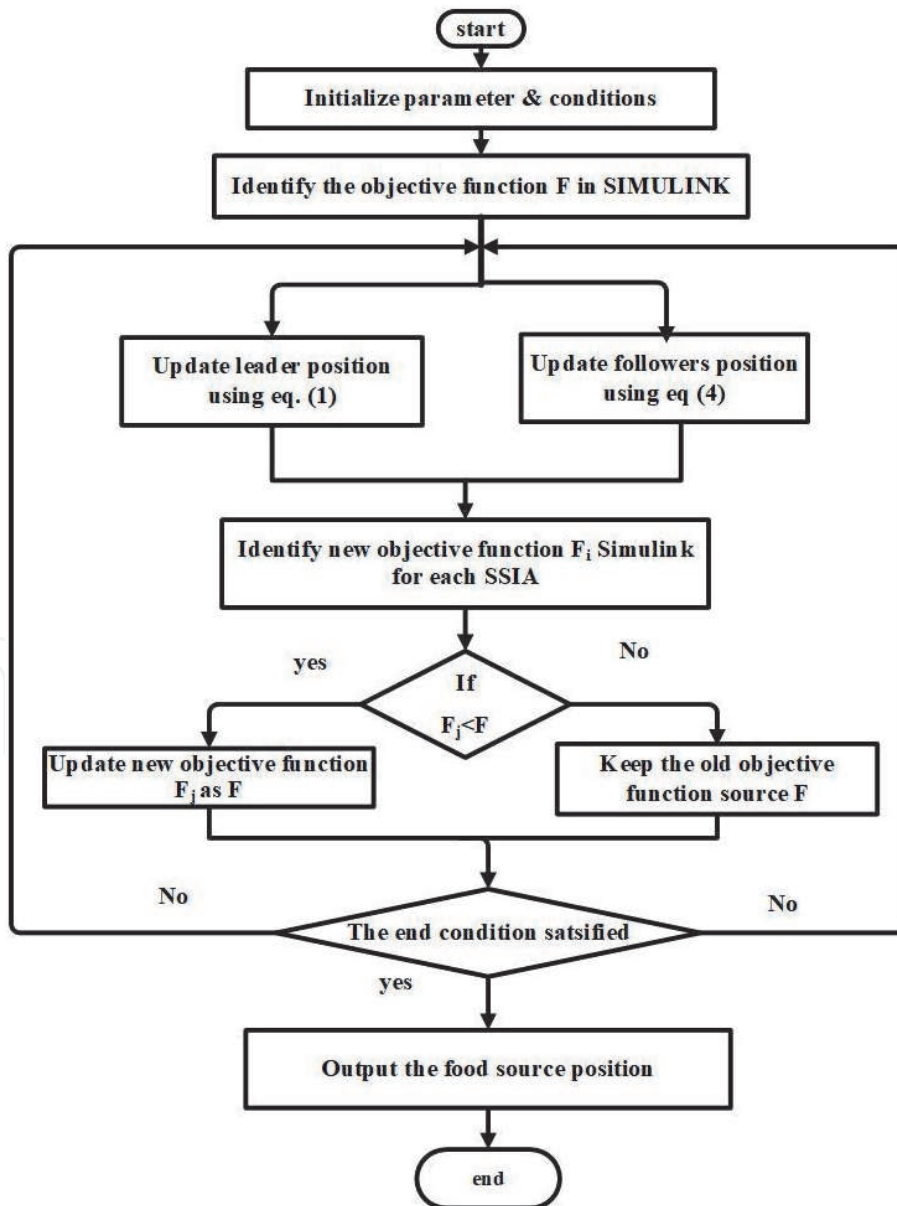


Figure 4.
 The flowchart of Salp swarm inspired algorithm.

3. Concept droop control

The ability of the inverter device is one of the fundamental objectives on which the wireless structure relies to regulate the output voltage and frequency while sharing the power and reactive demands. A key to wireless techniques is the use of droop control [33]. This is widely used in conventional power generation systems. A feature of this is that an external communication mechanism between inverters is not needed. In addition, its simple structure, based solely on the local voltage and current data, makes it possible for plug-and-play operations. The importance of droop control power in the island mode becomes obvious when it is possible to provide energy sharing across all units without the need to communicate with other units [3]. This method is built on the droop control of synchronous generators. The active and reactive power of each DG is determined with its nominal capacity and the droop coefficient. This is achieved by changing the droop coefficient, which increases the output resistance of the DG inverters, to regulate the amount of energy injected per DG on the grid. The output voltage and frequency of the inverter is controlled based on the reference active and reactive power of DGs, so the Q-V and P-f droop controllers are usually good candidates [34]. Therefore, the active power will be controlled according to the phase angle, whereas the voltage difference will regulate the reactive power. **Figure 5** demonstrates the relationship between P- ω and Q-V.

In the case of islands, the essential feature of droop control is to control the output power to achieve good power-sharing between transformers. This topology of the three-layer microgrid control strategy with its components will be addressed in detail in the following subsections.

3.1 Power circuit

In the power circuit, four components are used the three-phase VSI, the filter for resistive-inductive-capacitive (RLC), the inductor coupling (L_2), and the three-phase load.

3.2 Droop control

Droop control is a control technique that is usually applied to generators to allow parallel generators to be controlled by the microgrid. The relationship is

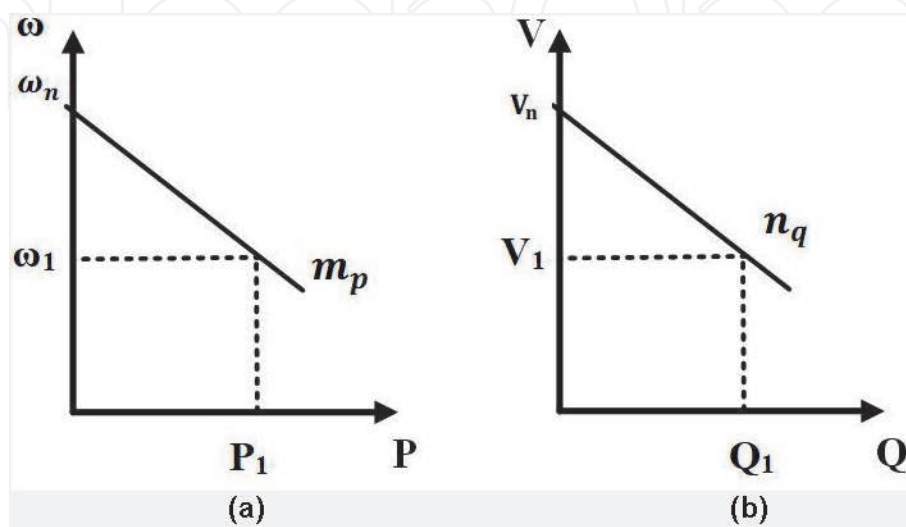


Figure 5. P- ω and Q-V droop control curves [34].

concentrated between the active power and the frequency and the reactive power and the voltage. Using the output voltage (ν_0) and output current (I_0) to calculate the active power (p) and the reactive power (q) before the filter, V_0 and I_0 are transformed to the dq reference frame for the calculation of (p and q) using below Equation [8, 35]:

$$p = \nu_{0d}I_{0d} + \nu_{0q}I_{0q} \quad (5)$$

$$q = \nu_{0d}I_{0q} + \nu_{0q}I_{0d} \quad (6)$$

where

ν_{0d} : the output voltage on the d reference frame.

ν_{0q} : the output voltage on the q reference frame.

I_{0d} : the output current on the d reference frame.

I_{0q} : the output current on the q reference frame.

P : the active power before the filter.

Q : the reactive power before the filter.

For enhancement, the p and q pass into a low pass filter and are renamed as P and Q . P and Q are determined in accordance with the following equation:

$$P = \frac{\omega_c}{S + \omega_c} (\nu_{0d}I_{0d} + \nu_{0q}I_{0q}) \quad (7)$$

$$Q = \frac{\omega_c}{S + \omega_c} (\nu_{0d}I_{0q} + \nu_{0q}I_{0d}) \quad (8)$$

where

ω_c : the cut-off frequency of low-pass filters.

S : the Laplace transform parameter.

P : the measured active power.

Q : the measured reactive power.

After calculating P and Q , the reference angular frequency ω and reference voltage V will be calculated using the equation below:

$$\omega = \omega_n - m_p * P \quad (9)$$

$$V = V_n - n_q * Q \quad (10)$$

where

ω : the reference angular frequency.

V : the reference voltage.

ω_n : the constant coefficients of frequency characteristics.

V_n : the constant coefficients of voltage characteristics.

m_p and n_q : the droop coefficients.

3.3 Voltage: current controller

An input to the voltage controller to find the reference current (I_i^*) will be the reference voltage and frequency. The voltage controller output I_i^* will feed the current controller. The current controller output (V^*) feeds the Pulse Width Modulation (PWM). The output of PWM is used to regulate VSI. I_i^* and V^* are determined by the equations below [8]:

$$I_i^* = -\omega C_f V_o^* + k_{pv} (V_o^* - V_o) + \frac{K_{iv}}{s} (V_o^* - V_o) \quad (11)$$

$$V^* = -\omega L_f I_i + k_{pc} (I_i^* - I_i) + \frac{k_{ic}}{S} (I_i^* - I_i) \quad (12)$$

where

L_f is the coupling inductor.

S is the Laplace transform parameter.

The voltage and current are controlled through the use of the PI controller. The gains of the PI controller and droop coefficients need to be exactly calculated. To determine PI gains and droop coefficients, there are many methods used, such as the trial and error method and the root locus method. However, these methods do not deal with the complicated nonlinear framework, such as microgrids, or even assess the controller's exact gains. Several studies are attempting to solve this issue because of the relevance of calculating PI gains and drop coefficients. So, the SSIA will be applied to obtain PI gains and drop coefficients.

4. SSIA application in microgrids

The proposed SSIA technology will be used to determine the optimum control parameters and drop control coefficients. SSIA determines the control parameters and droop coefficients (K_{p1} , K_{i1} , K_{p2} , K_{i2} , K_{p3} , K_{i3} , K_{p4} , K_{i4} , n_q , m_p) for the realization of minimized voltage and frequency fluctuations. Every optimization technique requires an objective function to perform its assigned task.

The objective function is designed to minimize the error between the calculated and expected voltage. Integral of absolute error (IAE), integral of square error (ISE), integral of time absolute error (ITAE), integral of time square error (ITSE) are the four types of error benchmark objective functions [36]. ITAE is the most widely used feature in literature for reducing control objectives. This is because ITAE aims for easier implementation and provides improved efficiency compared to its rivals. The ITSE and ISE are aggressive criteria and produce unrealistic assessments due to squaring of the mistake made. In contrast to the ITAE, the IAE is also an ineffective choice, reflecting reasonable a more practical error-index due to the time-multiplying error feature. ITAE mathematically explains the equation below:

$$ITAE = \int_0^{\infty} t \cdot |e(t)| \cdot dt \quad (13)$$

where

ITAE: integral of time absolute error.

t: time.

e: error.

The multi-objective function is used in this case study to recognize both the frequency and voltage errors via the property of the accumulative sum. **Figure 6** illustration the test system diagram consists of two solar PV array systems (SPVAS), a DC-DC boost converter, two battery stations (BSs), a supercapacitor (SC), a three-phase VSI, a load, and a transmission line [31]. Owing to their fast charging and discharging characteristics, supercapacitors are also used to boost the microgrid's dynamic response. The DC-DC boost converter is fitted with maximum power point tracking (MPPT) based on incremental conductance (INC) to control the DC voltage of the SPVAS output terminals. **Table 1** reviews the parameters of the test system (islanded microgrid model) [8]. The detailed comparative analysis is given in **Table 2** for three optimization techniques. The findings indicate that SSIA

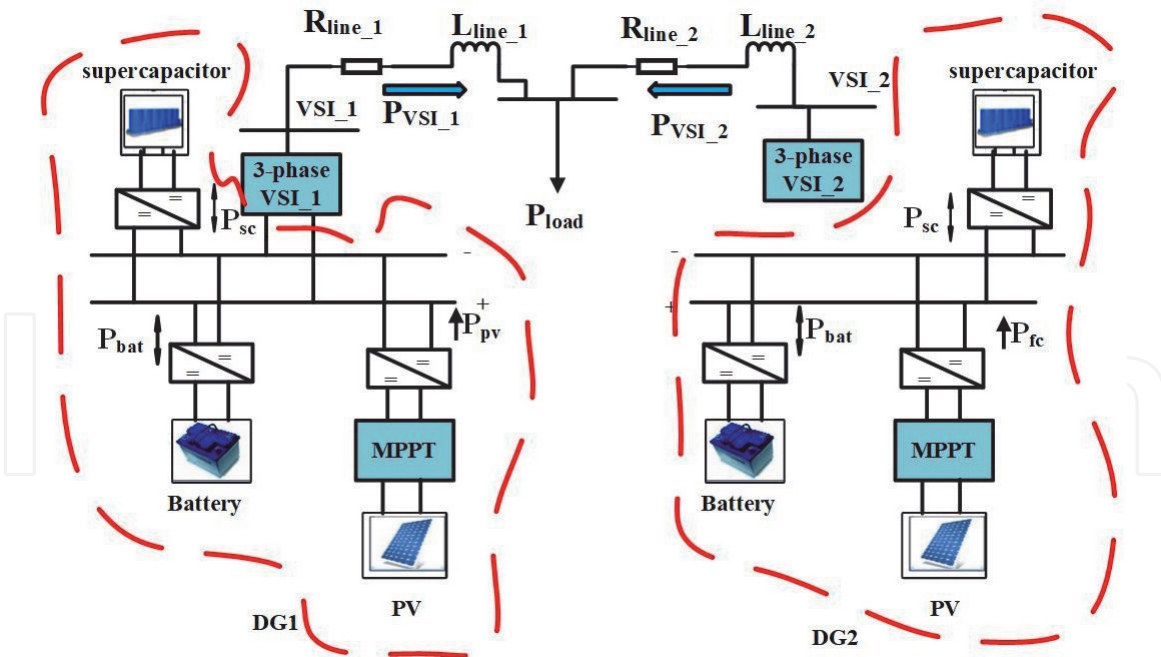


Figure 6.
 Test system diagram [31].

Parameter	Value	Parameter	Value
V_{base}	380 V	ω_n	1 p.u.
S_{base}	100 kVA	V_n	1 p.u.
ω_{base}	314 rad/sec	R_{line1}	0.14 p.u.
L_f	0.95×10^{-3} p.u.	L_{line1}	2.1×10^{-3} p.u.
C_f	35×10^{-6} p.u.	R_{line2}	0.2 p.u.
R_f	0.067 p.u.	L_{line2}	3.5×10^{-3} p.u.
L_c	0.23×10^{-3} p.u.	P_{load}	70×10^3
R_c	0.02 p.u.	ω_c	0.1 p.u.
T_s	5.144×10^{-6} sec	Frequency of PWM	10 kHz
Power of PV	109.88 kW	Capacitance of supercapacitor	29 F
Power of battery	56 kW		

Table 1.
 Test system parameters [8].

	SSA	PSO	ABC
Objective function	10.25×10^6	12.66×10^6	18.460×10^6
K_{p1}	0.691433	0.557908	0.641502
K_{i1}	311.4964	475.0824	530.0400
K_{p2}	0.548548	0.513765	0.470766
K_{i2}	543.6527	565.1678	349.2290
K_{p3}	11.27808	13.09909	12.22560
K_{i3}	13879.68	12410.52	6358.140
K_{p4}	10.25541	13.05646	9.003440
K_{i4}	14414.39	11132.63	13267.80

	SSA	PSO	ABC
n_q	0.272247	0.225909	0.266158
m_p	0.014868	0.009724	0.015636
Time Taken (min)	207.2686	219.1358	224.4803

Table 2.
Results of the applied three optimization techniques.

succeeded with minimal voltage and frequency errors in achieving the assigned control task. Three alternative optimization methods (SSIA, Particle Swarm Optimization (PSO), and ABC) are used to validate the quality of SSIA for a fair comparison.

5. Results of simulations

On a microgrid test device, well-tuned controllers via SSIA are equipped to confirm the power-sharing between multiple sources as well as the voltage and frequency regulation. The two types of load: constant and continuous change loads are considered in this study with RERs variability such as (variable irradiance and temperature).

5.1 Case I: islanding mode with fixed cyclic load variations scenario (IMFCLVS)

In this case, for islanded MG with a 70 kW (0.7p.u.) constant load, RERs variability (variable solar irradiance and temperature) is regarded. The ramp-up/

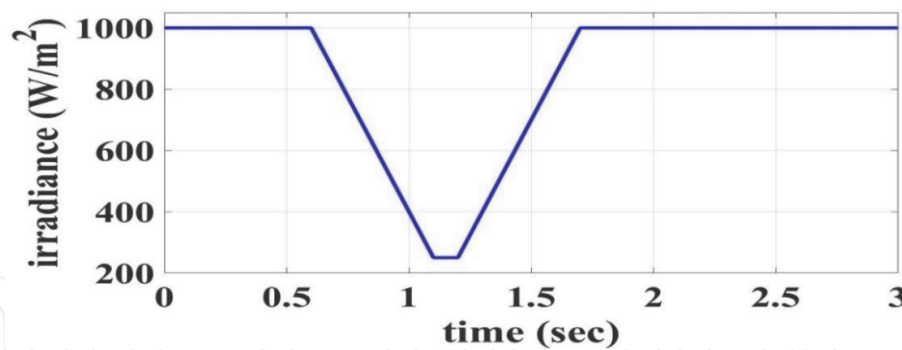


Figure 7.
Solar irradiance variation pattern for all applied scenarios.

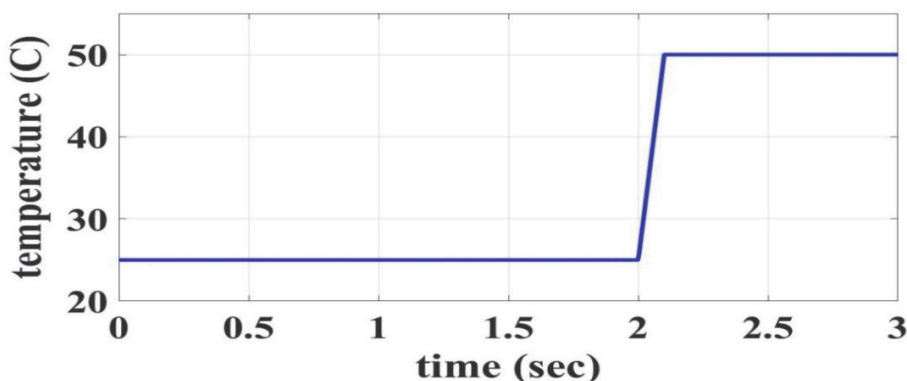


Figure 8.
Solar temperature variation for all applied scenarios.

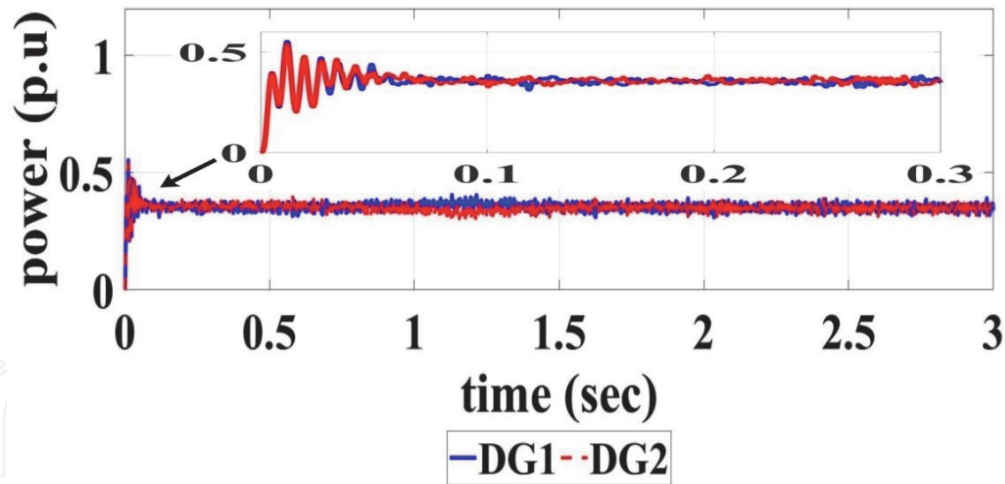


Figure 9.
 Active powers generated by two DGs IMFCLVS scenario.

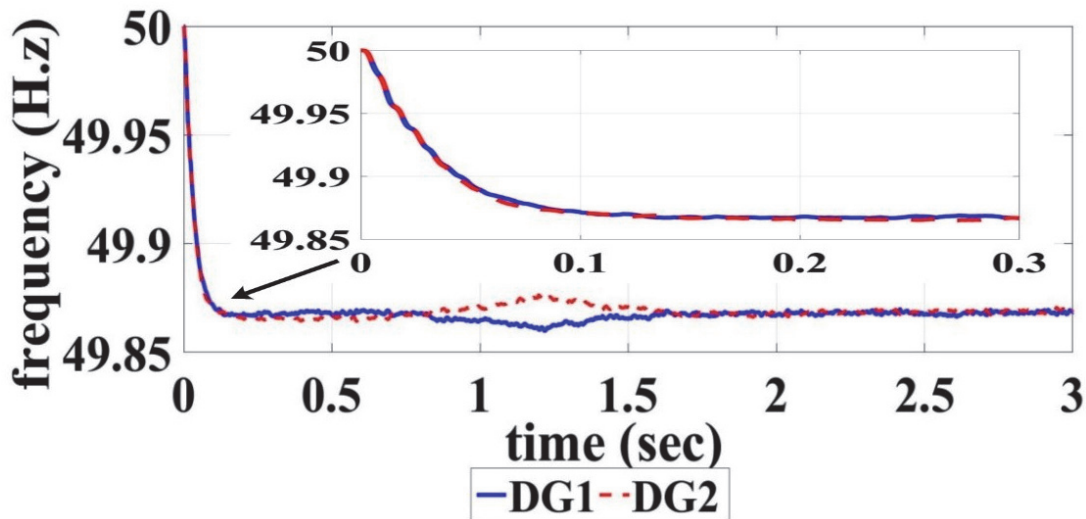


Figure 10.
 Inverter frequency of IMFCLVS scenario.

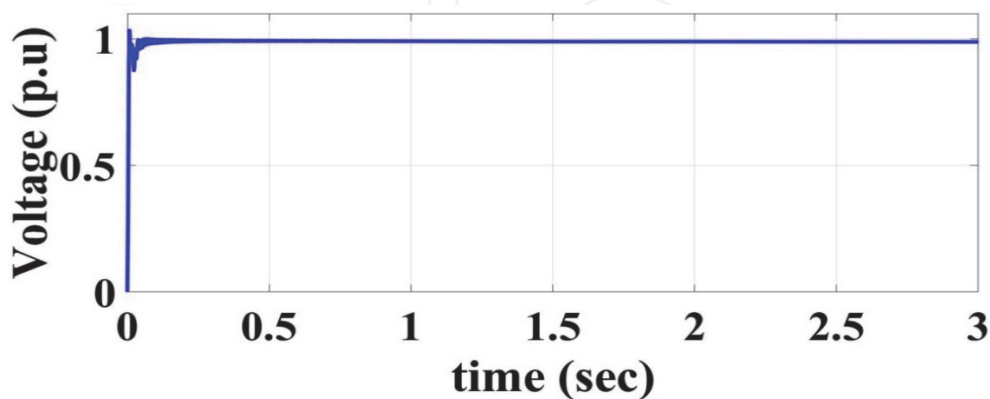


Figure 11.
 Voltage magnitude of IMFCLVS scenario.

down solar irradiance from 1000 W/m² to 250 W/m² is expressed in **Figure 7**. **Figure 8** establishes the temperature variation between 25°C and 50°C. For each source, the dynamic active power response is represented in **Figure 9**. It should be noted that for both sources, the active power is almost equal (0.35 p.u.), which confirms successful power-sharing. Remarkably, it is observed that solar radiation

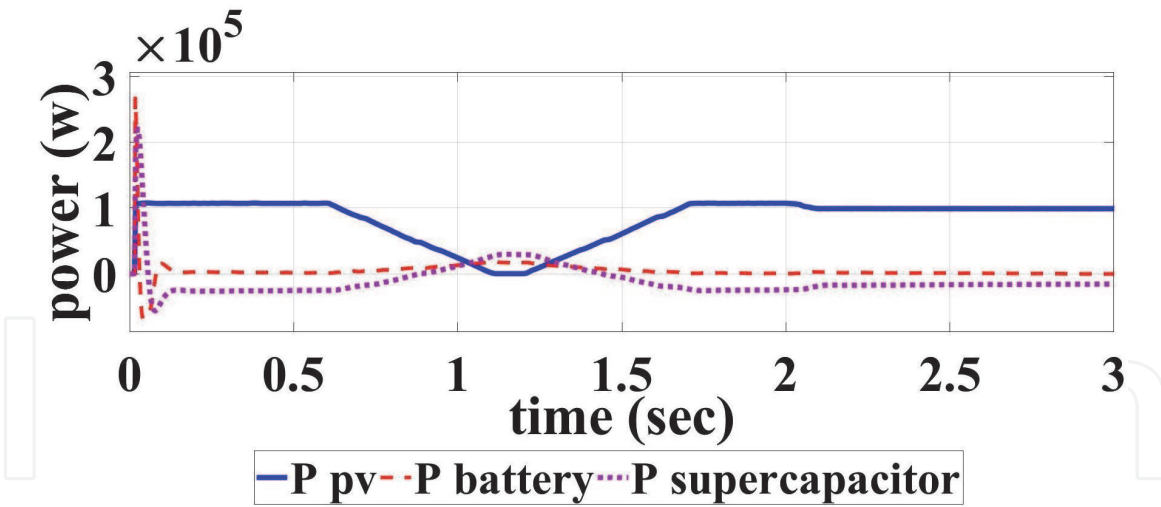


Figure 12.
Powers of SPVAs, BSs, and SC in IMFCLVS scenario.

and temperature fluctuations do not impact power-sharing because the total power fed to the DC bus is constant due to the mechanism of energy management. **Figures 10** and **11** indicate the frequency and voltage responses during the applied case. **Figure 12** shows the process of energy management among the multi-sources of MG (SPVAs, BS, and SC). It is clear from the findings that the droop control strategy based on SSIA dealt successfully with the variability of RERs.

5.2 Case II: islanding mode with continuous cyclic load variations scenario (IMCCLVS)

The microgrid is operated in islanding mode with continuous cyclic load variations under the variability of RERs as kW (0.7 p.u.) from 0 to 0.3 sec, then the load value increased to 110 kW (1.1 p.u.) at 0.3–0.7 sec, then the load value returned to 70 kW (0.7 p.u.) at 0.7–1.2 sec at the end of the load cycle. **Figure 13** shows that an equivalent amount of active power is injected into MG by each DG. The rate of power change is notably almost the same as the rate of load change, remarkably. **Figures 14** and **15** denote the transient response of frequency and voltage during the IMCCLVS scenario, respectively. Strikingly, **Figures 14** and **15** show that the frequency response indicates that the rate of power change is highly influenced by the frequency response, while the voltage is slightly affected. Additionally,

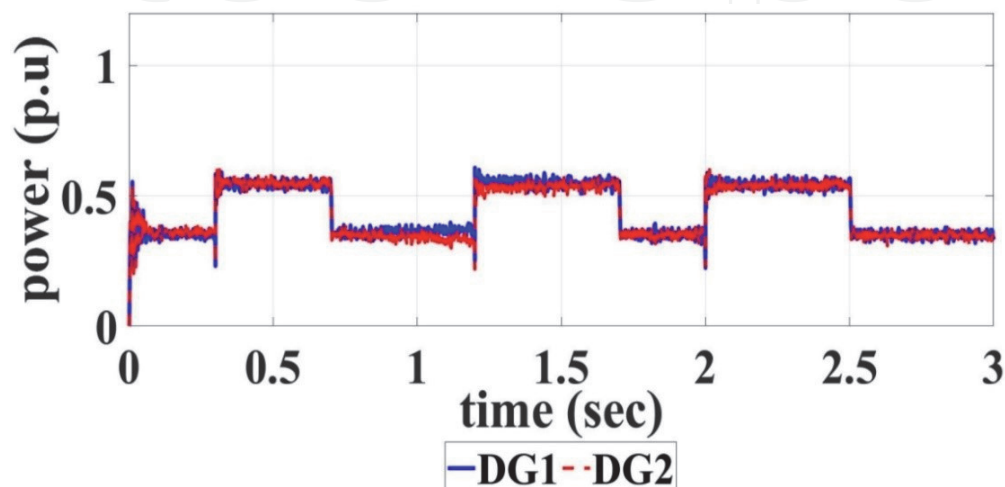


Figure 13.
Active powers generated by DGs in IMCCLVS scenario.

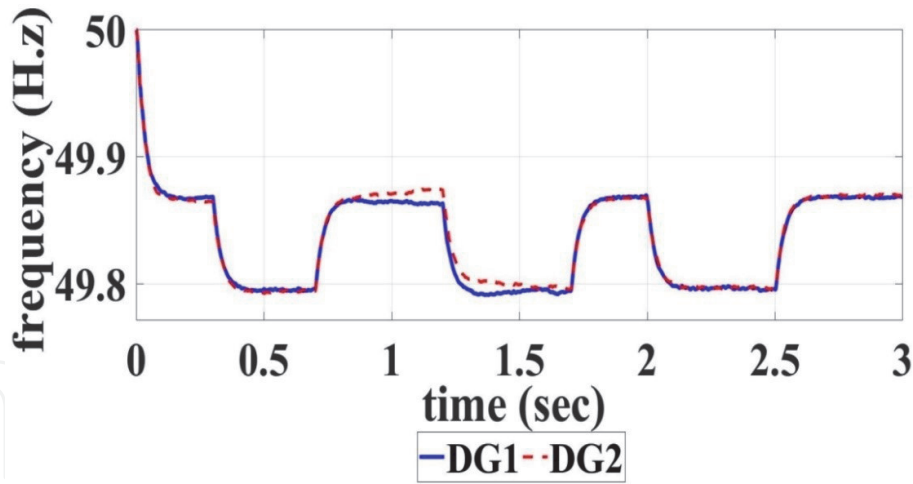


Figure 14.
Inverter frequency of IMCCLVS scenario.

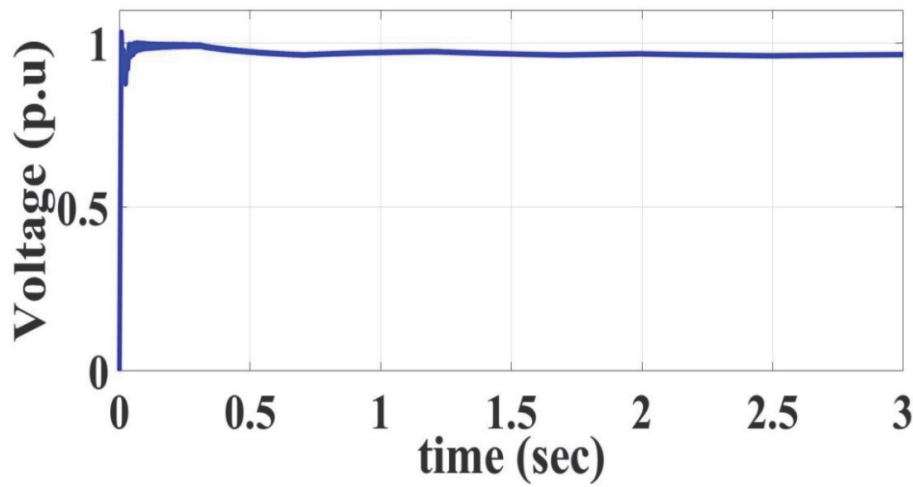


Figure 15.
Voltage magnitude IMCCLVS scenario.

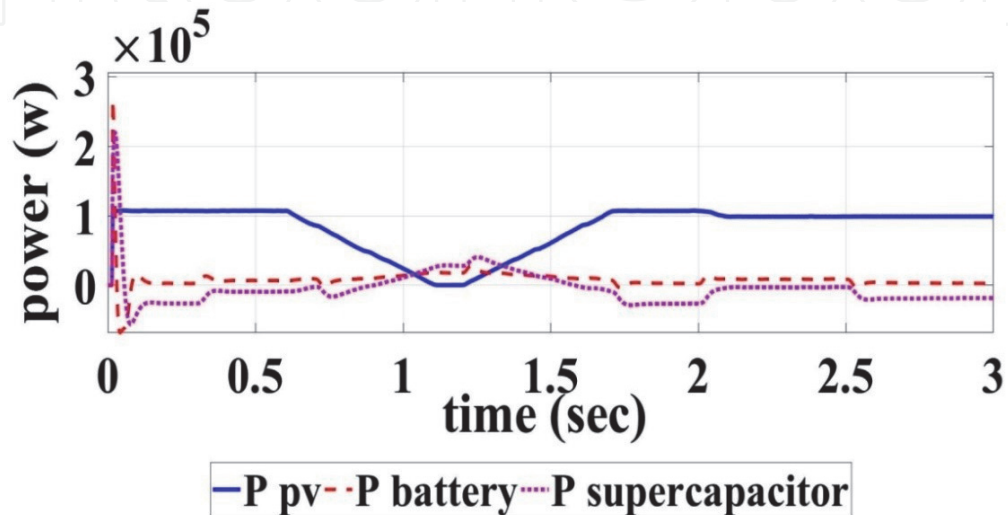


Figure 16.
Powers of SPVAs, BSs, and SC in IMCCLVS scenario.

Figure 16 demonstrates how SPVAs, BSs, and SC interact in dynamism with each other to preserve the continuity of supply.

6. Conclusions

In this chapter, an optimal SSIA-based voltage and frequency control and the power-sharing scheme was presented for inverter-dependent DG units in an island microgrid. Two sources and each source of a microgrid test system are available. The solar PV array, supercapacitor and battery station are included. To determine the gains of the PI controllers and coefficients of the droop control system, the SSIA is used. The cost function includes four forms: IAE, ISE, ITAE, and ITSE. The best solution is found when implementing ITAE as an objective function. By comparing three different types of optimization techniques (SSIA, PSO and ABC) applied to the microgrid scheme, the quality of SSIA as an optimization method was verified. In two cases, the achieved gains of PI controllers and droop control coefficients (K_{p1} , K_{i1} , K_{p2} , K_{i2} , K_{p3} , K_{i3} , K_{p4} , K_{i4} , n_q , m_p) are implemented in the system. Fixed load and slow and fast changes are considered in the proposed cases, as well as abrupt variations in both renewable energy supplies and loads. The results of the simulation indicated that the power-sharing depends on SSIA between the parallel DGs and the droop control strategy. The frequency deviation is within the acceptable range and the DGs are easily followed by changes in load with a good dynamic response.

Conflict of interest

The authors have no affiliation with any organization with a direct or indirect financial interest in the subject matter discussed in the manuscript.

Author details

Mohamed A. Ebrahim^{1*}, Reham M. Abdel Fattah², Ebtisam M. Saied^{1,3},
Samir M. Abdel Maksoud¹ and Hisham El Khashab²


¹ Electrical Engineering Department, Faculty of Engineering at Shoubra, Benha University, Cairo, Egypt

² Power Electronics and Energy Conversion Department, Electronics Research Institute, Cairo, Egypt

³ Electrical Engineering Department-High Technological Institute (HTI) 10th of Ramadan City, Egypt

*Address all correspondence to: mohamed.mohamed@feng.bu.edu.eg

IntechOpen

© 2021 The Author(s). Licensee IntechOpen. This chapter is distributed under the terms of the Creative Commons Attribution License (<http://creativecommons.org/licenses/by/3.0>), which permits unrestricted use, distribution, and reproduction in any medium, provided the original work is properly cited. 

References

- [1] Jumani TA, Mustafa MW, Rasid MM, Mirjat NH, Leghari ZH, Salman Saeed M. Optimal voltage and frequency control of an islanded microgrid using grasshopper optimization algorithm. *Energies* 2018;11. <https://doi.org/10.3390/en11113191>.
- [2] Khaledian A, Golkar MA. Analysis of droop control method in an autonomous microgrid 2017;15:371–7.
- [3] Tayab UB, Roslan MA Bin, Hwai LJ, Kashif M. A review of droop control techniques for microgrid. *Renew Sustain Energy Rev* 2017;76:717–27. <https://doi.org/10.1016/j.rser.2017.03.028>.
- [4] Goodarzi HM, Kazemi MH, Kazemi MH. An optimal autonomous microgrid cluster based on distributed generation droop parameter optimization and renewable energy sources using an improved grey wolf optimizer. *Eng Optim* 2017;0:1–21. <https://doi.org/10.1080/0305215X.2017.1355970>.
- [5] Zeng Z, Yang H, Zhao R. Study on small signal stability of microgrids: A review and a new approach. *Renew Sustain Energy Rev* 2011;15:4818–28. <https://doi.org/10.1016/j.rser.2011.07.069>.
- [6] Shokoohi S, Bevrani H. An Intelligent Droop Control for Simultaneous Voltage and Frequency Regulation in Islanded Microgrids. *IEEE Trans Smart Grid* 2013;4:1505–13. <https://doi.org/10.1016/j.ijepes.2014.07.024>.
- [7] Zeng X, Tang C, Wang W, Tang X. Analysis of microgrid inverter droop controller with virtual output impedance under non-linear load condition. *IET Power Electron* 2014;7:1547–56. <https://doi.org/10.1049/iet-pe.1.2013.0407>.
- [8] Kohansal M, Gharehpetian GB, Abedi M. An optimization to improve voltage response of VSI in islanded Microgrid considering reactive power sharing. 2012 2nd Iran Conf Renew Energy Distrib Gener ICREDG 2012 2012:127–31. <https://doi.org/10.1109/ICREDG.2012.6190447>.
- [9] Aljarah I. Grasshopper optimization algorithm for multi-objective optimization problems 2017. <https://doi.org/10.1007/s10489-017-1019-8>.
- [10] Tsai C, Eberle W, Chu C. Knowledge-Based Systems Genetic algorithms in feature and instance selection. *Knowledge-Based Syst* 2013;39:240–7. <https://doi.org/10.1016/j.knosys.2012.11.005>.
- [11] Heidari AA, Mirjalili S, Faris H, Aljarah I, Mafarja M, Chen H. Harris hawks optimization: Algorithm and applications. *Futur Gener Comput Syst* 2019;97:849–72. <https://doi.org/10.1016/j.future.2019.02.028>.
- [12] Mirjalili S, Gandomi AH, Mirjalili SZ, Saremi S, Faris H, Mirjalili SM. Salp Swarm Algorithm: A bio-inspired optimizer for engineering design problems. *Adv Eng Softw* 2017;114:163–91. <https://doi.org/10.1016/j.advengsoft.2017.07.002>.
- [13] Abbassi R, Abbassi A, Asghar A, Mirjalili S. An efficient salp swarm-inspired algorithm for parameters identification of photovoltaic cell models An efficient salp swarm-inspired algorithm for parameters identification of photovoltaic cell models. *Energy Convers Manag* 2018;179:362–72. <https://doi.org/10.1016/j.enconman.2018.10.069>.
- [14] Hegazy AE, Makhlof MA, El-Tawel GS. Improved salp swarm algorithm for feature selection. *J King Saud Univ - Comput Inf Sci* 2018. <https://doi.org/10.1016/j.jksuci.2018.06.003>.

- [15] Saremi S, Mirjalili S, Lewis A. Grasshopper Optimisation Algorithm: Theory and application. *Adv Eng Softw* 2017;105:30–47. <https://doi.org/10.1016/j.advengsoft.2017.01.004>.
- [16] Mirjalili S, Lewis A. The Whale Optimization Algorithm. *Adv Eng Softw* 2016;95:51–67. <https://doi.org/10.1016/j.advengsoft.2016.01.008>.
- [17] Ebrahim MA, Osama A, Kotb KM, Bendary F. Whale inspired algorithm based MPPT controllers for grid-connected solar photovoltaic system. *Energy Procedia* 2019;162:77–86. <https://doi.org/10.1016/j.egypro.2019.04.009>.
- [18] Mafarja MM, Mirjalili S. Hybrid Whale Optimization Algorithm with simulated annealing for feature selection. *Neurocomputing* 2017;260:302–12. <https://doi.org/10.1016/j.neucom.2017.04.053>.
- [19] Mirjalili S. Moth-flame optimization algorithm: A novel nature-inspired heuristic paradigm. *Knowledge-Based Syst* 2015;89:228–49. <https://doi.org/10.1016/j.knosys.2015.07.006>.
- [20] Mirjalili S, Mirjalili SM, Lewis A. grey wolf. *Adv Eng Softw* 2014;69:46–61. <https://doi.org/10.1016/j.advengsoft.2013.12.007>.
- [21] Ahmed Ebrahim M, Mohamed RG. Comparative Study and Simulation of Different Maximum Power Point Tracking (MPPT) Techniques Using Fractional Control and Grey Wolf Optimizer for Grid Connected PV System with Battery. *Electr Power Convers* 2019;2016:1–14. <https://doi.org/10.5772/intechopen.82302>.
- [22] Soued S, Ebrahim MA, Ramadan HS, Becherif M. Optimal blade pitch control for enhancing the dynamic performance of wind power plants via metaheuristic optimisers. *IET Electr Power Appl* 2017;11:1432–40. <https://doi.org/10.1049/iet-epa.2017.0214>.
- [23] Mirjalili S. The ant lion optimizer. *Adv Eng Softw* 2015;83:80–98. <https://doi.org/10.1016/j.advengsoft.2015.01.010>.
- [24] Aouchiche N, Aitcheikh MS, Becherif M, Ebrahim MA. AI-based global MPPT for partial shaded grid connected PV plant via MFO approach. *Sol Energy* 2018;171:593–603. <https://doi.org/10.1016/j.solener.2018.06.109>.
- [25] Ebrahim MA, Becherif M, Abdelaziz AY. Dynamic performance enhancement for wind energy conversion system using Moth-Flame Optimization based blade pitch controller. *Sustain Energy Technol Assessments* 2018;27:206–12. <https://doi.org/10.1016/j.seta.2018.04.012>.
- [26] Ali AM, Ebrahim MA, Moustafa Hassan MA. Automatic voltage generation control for two area power system based on particle swarm optimization. *Indones J Electr Eng Comput Sci* 2016;2:132–44. <https://doi.org/10.11591/ijeecs.v2.i1.pp132-144>.
- [27] Ebrahim MA, Mostafa HE, Gawish SA, Bendary FM. Design of decentralized load frequency based-PID controller using stochastic particle swarm optimization technique. 2009 Int Conf Electr Power Energy Convers Syst EPECS 2009 2009.
- [28] Mirjalili S. Dragonfly algorithm: a new meta-heuristic optimization technique for solving single-objective, discrete, and multi-objective problems. *Neural Comput Appl* 2016;27:1053–73. <https://doi.org/10.1007/s00521-015-1920-1>.
- [29] Mirjalili S, Gandomi AH, Mirjalili SZ, Saremi S, Faris H, Mirjalili SM. Salp Swarm Algorithm: A bio-inspired optimizer for engineering design problems. *Adv Eng Softw* 2017;114:163–91. <https://doi.org/10.1016/j.advengsoft.2017.07.002>.
- [30] Abbassi R, Abbassi A, Heidari AA, Mirjalili S. An efficient salp

swarm-inspired algorithm for parameters identification of photovoltaic cell models. *Energy Convers Manag* 2019;179:362–72. <https://doi.org/10.1016/j.enconman.2018.10.069>.

[31] Ebrahim MA, Fattah RMA, Saied EM, Maksoud SMA, El Khashab H. Real-Time Implementation of Self-Adaptive Salp Swarm Optimization-based Microgrid Droop Control. *IEEE Access* 2020;8:1–1. <https://doi.org/10.1109/access.2020.3030160>.

[32] Qais MH, Hasanien HM, Alghuwainem S. Enhanced salp swarm algorithm: Application to variable speed wind generators. *Eng Appl Artif Intell* 2019;80:82–96. <https://doi.org/10.1016/j.engappai.2019.01.011>.

[33] Lopes JAP, Moreira CL, Madureira AG. Defining control strategies for microgrids islanded operation. *IEEE Trans Power Syst* 2006;21:916–24. <https://doi.org/10.1109/TPWRS.2006.873018>.

[34] Zafari P, Zangeneh A, Moradzadeh M, Ghafouri A, Parazdeh MA. Various Droop Control Strategies in Microgrids. *Power Syst* 2020:527–54. https://doi.org/10.1007/978-3-030-23723-3_22.

[35] Ebrahim MA, Aziz BA, Nashed MNF, Osman FA. A Novel Hybrid-HHOPSO Algorithm based Optimal Compensators of Four-Layer Cascaded Control for a New Structurally Modified AC Microgrid. *IEEE Access* 2020. <https://doi.org/10.1109/ACCESS.2020.3047876>.

[36] Hussain KM, Zepherin RAR, Kumar MS, Kumar SMG. Comparison of PID Controller Tuning Methods with Genetic Algorithm for FOPTD System. *J Eng Res Appl* 2014;4:308–14.